New Horizons in Earth Reinforcement – Otani, Miyata & Mukunoki (eds)
© 2008 Taylor & Francis Group, London, ISBN 978-0-415-45775-0

Numerical analysis of fibre-reinforced granular soils

E. Ibraim
Department of Civil Engineering, University of Bristol, UK

K. Maeda
Department of Civil Engineering and Environmental, Nagoya Institute of Technology, Japan

ABSTRACT: Laboratory experimental tests of sand reinforced with discrete random flexible fibres show that fibre reinforcement could be an effective technique for improving their strength and deformation characteristics. The behaviour of fibre reinforced sand is influenced by many factors such as density and stress level, fibre type, content and orientation. A two dimensional DEM (Distinct Element Method) biaxial compression simulation of mixtures of sand and fibres is applied to understand how randomly distributed flexible fibres generate a bond within the soil and affect the kinematics of the granular matrix. Sand particles are modelled by rigid disks with conventional contact elements in DEM. The fibre element is modelled by connecting small circular particles with a bond contact algorithm, where the strength of the bond is fairly high. The specimens have been reinforced with different fibre fractions. The effect of fibre reinforcement is discussed.

1 INTRODUCTION

The concept of reinforcing soils by tension-resisting elements included in soil is widely accepted in geotechnical engineering practice. Traditional methods of earth reinforcement for embankments, earth-retaining structures and foundations use a large variety of continuous planar synthetic inclusions such as strips, fabrics or geotextiles (Koerner and Welsh, 1980). The reinforcement inclusions are normally oriented in a preferred direction, dependent on the geometry of the structure, the nature of the applied loads and the expected principal tensile strains in the soil. There has been much research on this topic over the last few decades. However, far less information is available on reinforcements with non-traditional inclusions, such as natural or synthetic short and flexible fibres randomly distributed.

Laboratory experiments show that the engineering behaviour of randomly distributed fibre reinforced soils is controlled by several parameters: stress level; fibre type, volume fraction, aspect ratio, modulus of elasticity, strength, orientation; and soil density, particle size, shape, gradation. The benefits of fibre reinforcement come from fibre-soil particle interaction. Modelling of fibre reinforcement effects has concentrated on prediction of the contribution of fibres to strength increase. For example, an attempt to describe the shear strength increase through consideration of soil/fibre interaction in a localised shear band by using a simple force-equilibrium model was made by Gray and Ohashi (1983), Jewell and Wroth (1987) – for oriented fibres – and Maher and Gray (1990) – for random distributed fibres. Using an energy-based homogenisation approach, a failure criterion was derived by Michalowski and Zhao (1996) while, more recently, Zornberg (2002) proposed a framework to predict failure of different soil types mixed with different fibre contents and fibre length/diameter ratios based on the superposition of the sand-fibre effects. Diambra et al. (2007) have shown that moist tamping technique produces specimens with 97% of fibres orientated within $\pm 45°$ to the horizontal.

In this paper a micromechanical approach is used in order to reveal the reinforcement mechanism of how randomly distributed flexible fibres with kinematics of the granular matrix. A two dimensional DEM (Distinct Element Method) (Cundall and Strack 1979) simulation of the mixture of sand and fibre is developed and numerical results under isotropic compression and shearing processes are presented and discussed in association with the observed experimental patterns.

2 EXPERIMENTAL FINDINGS

Published laboratory experimental test results, and pilot tests performed at Bristol (Ibraim and Fourmont 2006), show that reinforcement of sands with discrete random flexible fibres represents an effective

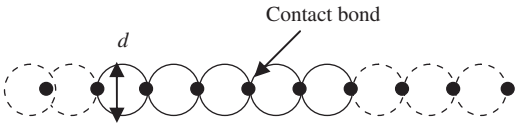

Figure 1. Typical model for fibres in DEM.

technique for improving their strength, ductility and reducing post-peak strength loss. Strength increase of the reinforced sand seems to be linear with the amount of fibres. Nevertheless, above some limiting fibre content, this increase seems to approach an asymptotic upper limit (Gray and Al-Refeai 1986, Murray et al. 2000). The amount of vertical dilation increases with the amount of fibres (Palmeira and Milligan 1989, Kaniraj and Havanagi 2001, Jewell and Wroth 1987, Shewbridge and Sitar 1989, Ibraim and Fourmont 2006).

Typically, sand reinforced with randomly distributed discrete fibres exhibits either curved-linear (for uniform, rounded sand) or bilinear (for well-graded or angular sands) failure envelopes (Gray and Ohashi 1983, Maher and Gray 1990). Above a threshold confining stress (critical confining stress, σ_{crit}) failure envelopes for the reinforced sand are parallel to the unreinforced sand envelope. Below the σ_{crit}, it is considered that the reinforcing mechanism is not fully mobilized and with the shearing process the fibres tend to slip or pull out.

Recent experimental results presented by Heineck et al. (2004) show that the fibre reinforcement seems to have no influence in the small strain domain.

3 DEM PROCEDURE

3.1 *Modelling of fibres and granular matrix*

The fibre was modelled by particles of diameter d connected by contact bond with tension and shear strengths and without rotation constraints like a hinge connection, as shown in Figure 1 (Ibraim et al., 2006). Since both strengths were considered to be fairly high, in this paper, fibre elements were flexible but were not allowed to break. The basic parameters for fibres are presented in Table 1.

The granular matrix is composed of rigid disks. The interaction between elements was modelled by contact elements (springs, dash-pots, sliders and non-extensional elements); these coefficients were introduced elsewhere by Maeda et al. (2003). Table 2 presents the parameters for the granular matrix.

3.2 *Sample preparation*

Figure 2 shows the fibre reinforced granular soil specimen model for the DEM. Gray and black balls represent granular matrix (approximately 1000 disks) and fibres, respectively. Bi-axial stresses are controlled by the movement of four boundary walls. After isotropic compression, the sample is sheared axially under constant strain-rate and lateral pressure.

In order to study the effect of the change in soil fabric due only to the imposed stress states, the specimens have been constructed under zero gravity condition. Initially fibre elements and matrix particles (void ratio of matrix phase: 0.24; $e_{max} = 0.27$, $e_{min} = 0.21$) were randomly generated. Then, all radii were multiplied

Table 1. Basic parameters for DEM simulations: fibres.

Parameter	Unit	Value
ρ_f	(Mg/m^3)	9.1
Diameter: d	(mm)	1($d/D_{max} = 0.1$)
Length: l	(mm)	150 ($l/D_{max} = 15$)
Aspect ratio: $\lambda = l/d$	(mm)	150

*$d =$ diameter, $l =$ length, $\lambda =$ aspect ratio ($\lambda = l/d$).

Table 2. Basic parameters for DEM simulations: granular matrix.

Parameter	Unit	Value
ρ_s	(Mg/m^3)	2.65
Shape of grain	–	circle
Grain size distribution		Gaussian distribution in weight
D_{max}	(mm)	10
D_{min}	(mm)	5
D_{50}	(mm)	7.1
C_u		1.3
C_g		1.1

*D_{max} = maximum grain size, D_{min} = minimum grain size, D_{50} = mean grain size, C_u = coefficient of uniformity (D_{60}/D_{10}), C_g = coefficient of gradation (D_{30}/D_{60} *D_{10}), ρ_s = density.

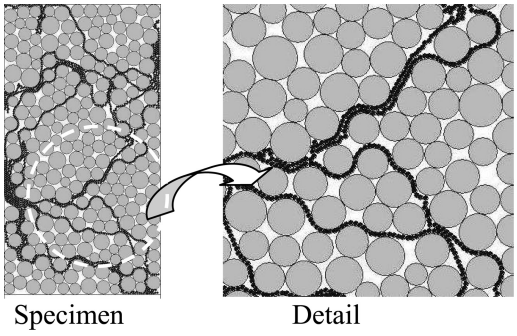

Figure 2. Example of fibre-reinforced constructed specimen for DEM simulation.

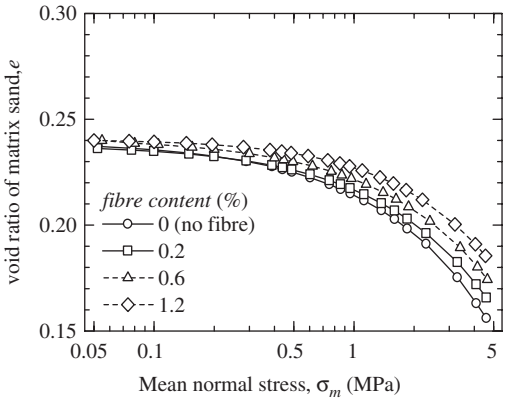

Figure 3. Typical results of isotropic compression tests analyzed by DEM on fibre-reinforced mixture: void ratio is obtained only from granular matrix phase.

gradually to the prescribed values in order to obtain an isotropic specimen. The detailed techniques for particle generation and density control of specimen are given by Maeda et al. (2003).

4 MACRO BEHAVIOURS ANALYZED

Figure 3 shows deformation behaviour of fibre-reinforced granular specimens under isotropic compression tests in a wide range of lateral pressure from 0.05 to 5 MPa. For pressures lesser than 0.5 MPa, the deformation responses for all specimens are almost identical. However, starting with 0.5 MPa, it is clearly that the specimen reinforced with higher fibre content shows a lower compressibility. For each fibre content, distinct normal compression lines are obtained and they tend to become parallel, as experimentally observed by Consoli et al. (2005).

Figure 4 shows deformation-failure behaviour of fibre-reinforced granular specimens analyzed. Different percentages by weight of matrix of fibre contents are used. All tests were conducted with constant lateral pressure σ_c of 0.1 MPa in x-axis direction and constant strain rate in y-axis direction.

The presence of fibres enhances the response of the reinforced mixture. The peak stress ratio, τ_m/σ_m, where τ_m is the maximum shear stress and σ_m the mean effective stress, increases with the amount of fibres. After an initial contractant phase, the simulations show a dilative volumetric response of the specimens. However, the dilation is not inhibited by the presence of fibres, but increases with the fibre content.

Figure 5 shows the dilatancy ratio evolution with the principal stress ratio for all the test simulations. The figure shows also Rowe's relationship (Rowe 1962)

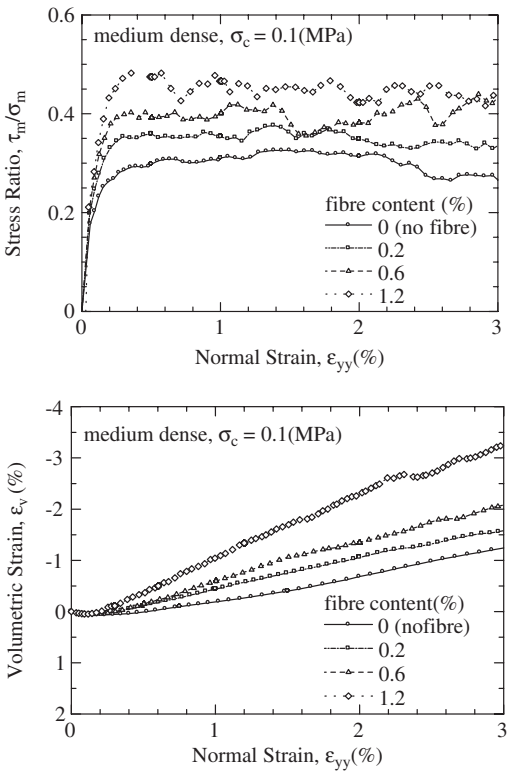

Figure 4. Typical results of biaxial compression tests given by DEM on fibre-reinforced mixture.

for an inter-particle friction angle, ϕ_μ, of 25°. There is no difference among the numerical results under contractant phase. Otherwise, the dilation phase shows different inclinations of the curves with the highest slope corresponding to the highest fibre content. The data diverge from Rowe's flow rule. These results may suggest that for fibre-reinforced granular materials there is no longer a unique flow rule which links the strength to the volumetric response.

5 MICRO OBSERVATIONS

5.1 *Fibre interactions during isotropic compression*

The averaged tensile stress computed for all the bond contacts on the fibres developed with the macro deformation under isotropic compression is plotted in Figures 6. A slight increase of the averaged tensile stress was recorded for σ_m values below 0.5 MPa. However, as can be observed in Figure 6, above 0.5 MPa of medium confining pressure, the averaged tensile stress increases remarkably. These results show that even if the specimens are undergoing isotropic

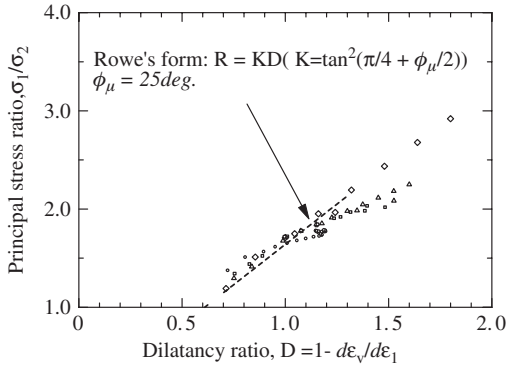

Figure 5. Stress – dilatancy ratio relations for the performed simulations (legend as given in Figure 4).

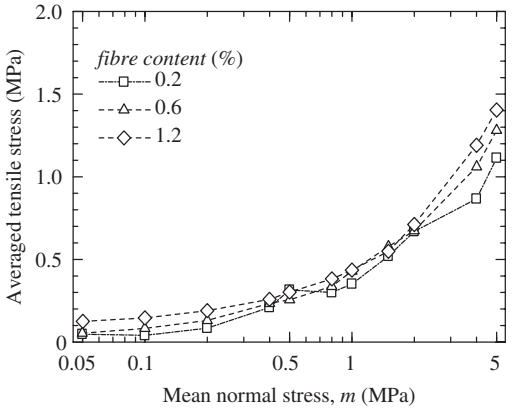

Figure 6. Averaged tensile stress in fibres developed with macro deformation under isotropic compression.

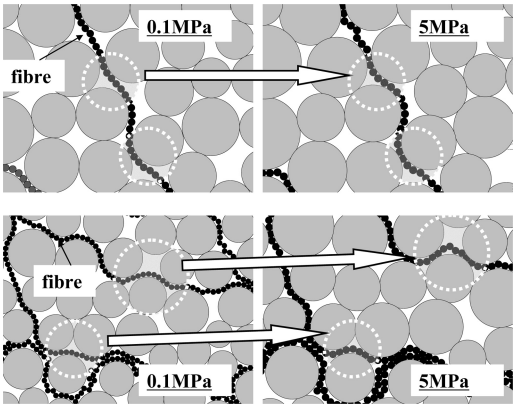

Figure 7. Change in configuration of fibre during isotropic compression from 0.1 MPa to 5 MPa.

compression, important tensile stresses are developing for the fibres. As the averaged tensile stress increases with the applied stress, for certain fibre types with relatively low individual tensile stress resistances, the breaking point can be reached. Extended and broken fibres have been found on isotropically compressed fibre reinforced specimens by Consoli et al. (2005). The variation of the fibre content does not seem to have a big influence on the computed averaged tensile stress.

It is interesting to note the change in configuration of fibres during isotropic compression, as we can observe changes in curvature of fibres at some local areas (Figure 7). For lower stress levels, the interaction mechanism between fibre and granular matrix in is not fully mobilized; otherwise it is induced by rearrangement of particles by applied higher stresses.

Figure 8 shows the spatial distribution of the tensile stress along the fibres located in the central area of the specimen (0.6% of fibre content) at the normal strain $\sigma_m = 5$ MPa. The distribution of the tensile stress appears to be random but highly non-homogeneous.

5.2 *Fibre interactions during shear*

The averaged tensile stress in the fibres developed with macro shear deformation is plotted in Figure 9. In the small and medium strain domains, ε_{yy} less than 0.2%, the initial tensile stress induced locally by the particle/fibre interaction during the isotropic compression phase remains unchanged; the interaction mechanism between the fibres and matrix is not mobilized and the behaviour of the composite appears to be dominated by the matrix properties. These results are in agreement with experimental observations presented by Palmeira and Milligan 1989, Jewell and Wroth (1987), and Heineck et al. (2004).

For axial strains higher than 0.2%, the averaged tensile stress in the reinforcement begins to increase. This trend appears to coincide also with the onset of the dilation phase of the mixed material. The tensile stress continues to increase well beyond the corresponding peak stress of the mixed material. As shown in Figure 9, higher fibre tensile stresses are mobilized in the specimens with higher fibre contents.

Figure 10 shows the spatial distribution of the tensile stress along the fibres located in the central area of the specimen (0.6% fibre content) at the normal strain $\varepsilon_{yy} = 2\%$. The distribution of the tensile stress appears to be highly non-homogeneous. The highest tensile stresses seem to be mobilized on fibres oriented towards the minor principal strain direction (tensile strain direction). The intensity of the tensile stress can be up to two times the averaged tensile stress. The beneficial effect of fibre reinforcement is higher when the fibres are oriented in the direction of the tensile strain, as experimentally observed by Gray and

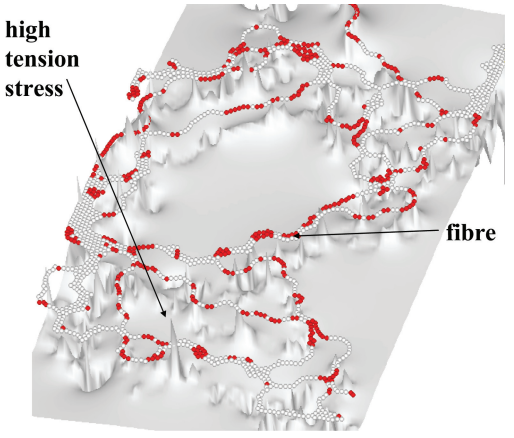

Figure 8. Spatial distribution of tensile stress in fibres in a zone cut in specimen: fibre content = 0.6% and $\sigma_m = 5$ MPa.

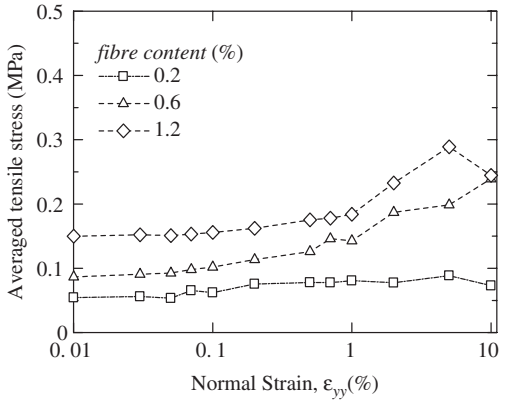

Figure 9. Averaged tensile stress in fibres developed with macro deformation under shearing.

Ohashi (1983), Jewell and Wroth (1987) among others. However, according to the results presented in the Figure 10, not all the horizontal oriented fibres are highly tensioned. Local micro fabric and local structural rearrangement may have an important effect on the interaction mechanism.

In order to assess the fabric change of the granular matrix during deformation, two fabric indexes N_cF_1 and N_cF_2 are examined. The numerical results are plotted in Figure 11. The geometry index N_c represents the coordination number, and F_1 and F_2 are principal values of the fabric tensor corresponding to the major principal direction (1) and minor principal direction (2), respectively. Here, major principal direction corresponds to y-axis. The coordination number represents the averaged number of contacts per particle and indicates the overall stability of the fabric. In general, N_c has been found to be mainly affected by the normal

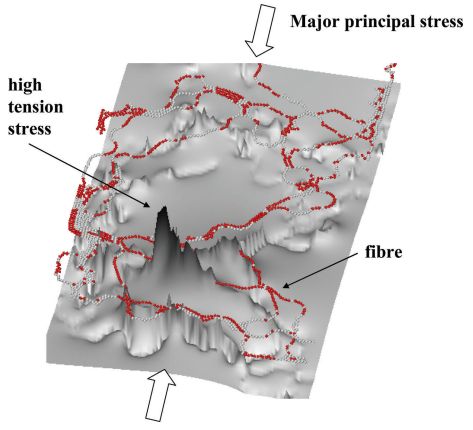

Figure 10. Spatial distribution of tensile stress in fibres in a zone cut in specimen: fibre content = 0.6% and at normal strain $\varepsilon_{yy} = 2.0\%$.

stress or stress ratio (Maeda et al. 2003; Maeda and Hirabashi, 2006). The major, F_1, and minor, F_2, principal values of fabric tensor are proposed by Satake (1982). Hence, F_1 and F_2 indicate the concentration intensity of normal direction of contact planes; the ratio F_1/F_2 means intensity of anisotropy. Maeda et al. (2003) pointed out that the directions of F_1 and F_2 agree with major and minor principal stress directions and the ratio F_1/F_2 is controlled by stress ratio and is independent of material properties and test conditions. Therefore, N_cF_1 and N_cF_2 could be considered as representative indices for fabric intensity over the principal directions.

As presented in Figure 11, for the case without fibres, the fabric intensities, N_cF_1 does not change but N_cF_2 decreases with macro deformation; this indicates a loss of contacts in lateral direction. For the cases with fibre, N_cF_1 increases for medium and large strains. This may explain, at macro-scale, the strength increase and the post-peak ductile behaviour experimentally observed for real fibre reinforced soils. In addition, the reduction of N_cF_2 reinforced is significantly smaller compared with the unreinforced case. These results suggest that the presence of fibres can prevent the loss of fabric in the direction of minor principal stress with beneficial consequences for mixed material.

The spatial distributions of the mean normal stress and deviator stress at the normal strain $\varepsilon_{yy} = 2\%$ for granular matrix phase located in the central area are shown in Figure 12 for an un-reinforced specimen and in Figure 13 for a reinforced specimen (0.6% of fibres content). In both cases, the stresses are distributed highly non-homogeneously. However, in the case of fibre reinforcement (Fig. 13), the vertical contact chains are much closer compared with the unreinforced specimen (Fig. 12). Higher mean normal

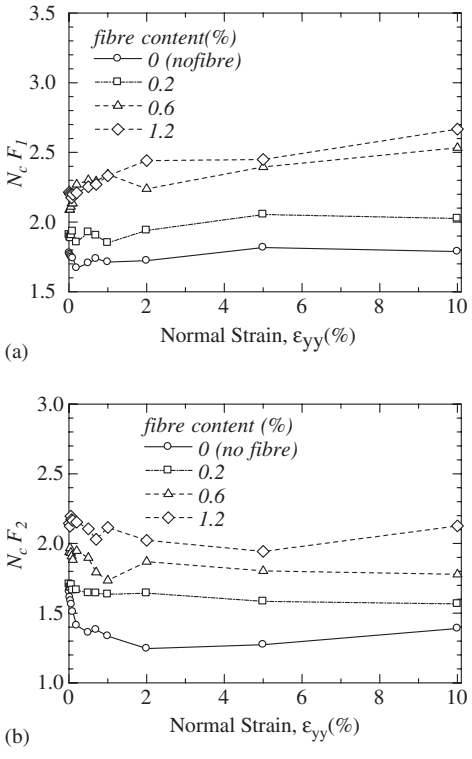

Figure 11. Contact fabric for granular matrix phase; (a) and (b) shows fabric in the direction of major and minor principal stress (y-axis and x-axis), respectively.

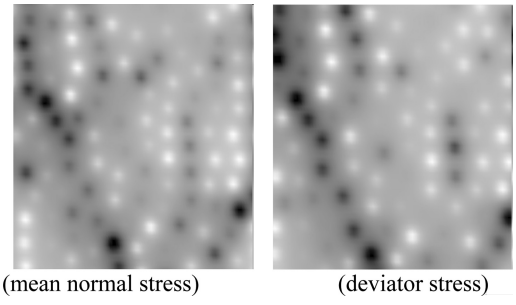

Figure 12. Stress distribution in micro zone for granular matrix phase in a zone cut in unreinforced specimen at normal strain $\varepsilon_{yy} = 2.0\%$ (stress scale in Pascals given on Figure 13).

and deviator stresses are localised on particles adjacent to the fibres, including horizontal directions.

6 CONCLUSIONS

A two dimensional DEM has been developed for the micromechanical analysis of mixtures of granular

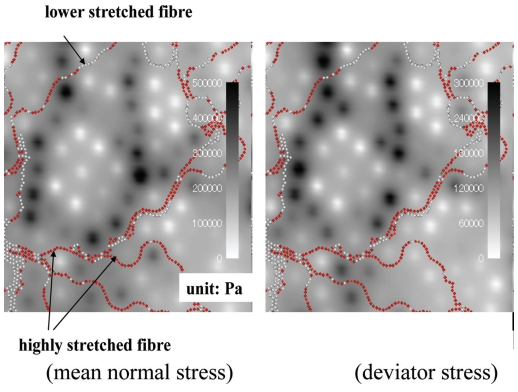

Figure 13. Stress distribution in micro zone for granular matrix phase in a zone cut in reinforced specimen at normal strain $\varepsilon_{yy} = 2.0\%$.

materials and flexible, discrete, randomly distributed fibres under isotropic compression and biaxial compression conditions. Evidently a two dimensional analysis implies that the fibres are completely separating the sand particles whereas the real material will have a continuity of stress transmission through the granular material provided by the third dimension.

Nevertheless, the DEM analysis describes well the experimentally observed strength increase induced by the presence of fibres. The dilatancy is equally affected by the amount of inclusions. The interaction mechanism does not seem to mobilise over the small and medium strain domains. Then, the fibre tensile stresses increase with the strain level and higher fibre tensile stresses are mobilized in specimens with higher fibre contents. It is also clearly shown that the highest tensile stresses are mobilized on fibres oriented towards the minor principal strain direction. However, local micro fabric and local structural rearrangement can affect the interaction mechanism and this was clearly shown for the isotropic compresses specimens. The presence of fibres also creates additional micro-confinement for the granular matrix.

REFERENCES

Consoli, N.C., Dal Toe Casagrande, & M. Coop, M.R. 2005. Effect of fibre reinforcement on the isotropic compression behaviour of a sand. *J. of Geotech. and Geoenv. Eng.* 131 (11): 1434–1436.

Cundall, P.A. 1971. A Computer Model for Simulation Progressive, Large Scale Movement in Blocky rock system. *Symp. ISRM*, Vol.2: 129–136.

Diambra, A., Russell, A.R., Ibraim, E. & Muir Wood, D. 2007, Determination of fibre orientation distribution in reinforced sand, *Geotechnique (accepted for publication).*

Gray, D.H. & Ohashi, H. 1983. Mechanics of fibre reinforcement in sand, *J. of Geotech. Eng.* 109 (3): 335–353.

Gray, D.H. & Al-Refeai, T.O. 1986. Behaviour of fabric – versus fiber-reinforced sand, *J. of Geotech. Eng.* 112 (8): 804–820.

Heineck, K.S., Coop, M.R. & Consoli, N.C. 2005. Effect of microreinforcement of soils from very small to large shear strains. *J. of Geotech. and Geoenv. Eng.* 131 (8): 1024–1033.

Ibraim, E. & Fourmont, S. 2006. Behaviour of sand reinforced with fibres. *Int. Geotech. Symposium*, March, Roma. 10 p.

Ibraim, E., Wood, D.M., Maeda, K. & Hirabashi, H. 2006. Fibre-reinforced granular soils behaviour, *International Symposium on Geotechnics of Particulate Media*: 443–448.

Jewell, R.A. & Wroth, C.P. 1987. Direct shear tests on reinforced sand. *Géotechnique* 37 (1): 53–68.

Kaniraj, S.R. & Havanagi, V.G. 2001. *J. of Geotech. and Geoenv. Eng.* 127 (7): 574–584.

Koerner, R.M. & Welsh, J.P. 1980. *Constructional and geotechnical engineering using synthetic fabrics.* New York; Chichester: Wiley.

Maeda, K., Hara Y. & Ohno, R. 2003. Interaction between piles with different skin roughness and granular ground by DEM. *VIIth International Conference on Computational Plasticity (COMPLAS)*, Barcelona, CD-ROM.

Maeda, K. & Hirabayashi, H. 2006. Influence of grain properties on macro mechanical behaviors of granular media by DEM, *Journal of Applied Mechanics, JSCE*: 623–630.

Maher, M.H. & Gray, D.H. 1990. Static response of sands reinforced with randomly distributed fibers. *J. of Geotech. Eng.* 116 (11): 1661–1677.

Michalowski, R.L. & Zhao, A. 1996. Failure of fiber-reinforced granular soils. *J. of Geotech. Eng.* 122 (3): 226–234.

Murray, J.J., Frost, J.D. & Wang, Y. 2000. Behaviour of sandy silt reinforced with discontinuous recycled fiber inclusions. *Transportation Research Record*, 1714: 9–17.

Palmeira, E.M. & Milligan, G.W.E. 1989. Large scale direct shear tests on reinforced soil. *Soils and foundations*, 29(1): 18–30.

Rowe, P.W. 1962. The stress Dilatancy relation for static equilibrium of an assembly of particles in contact. *Proc. R. Soc.* London, Ser. A., 269, 500–527.

Satake, M. 1982. Fabric tensor in granular materials. *IUTAM-Conference on Deformation and Failure of Granular Materials*: 63–68.

Shewbridge, S.E. & Sitar, N. 1989. deformation characteristics of reinforced sand in direct shear. *J. of Geotech. Eng.* 115 (8): 1134–1147.

Zornberg, J.G. 2002. Discrete framework for limit equilibrium analysis of fibre-reinforced soil. *Géotechnique*, 52 (8): 593–604.